A&A 436, 653–659 (2005)
DOI: 10.1051/0004-6361:20052726

Astronomy & Astrophysics

Properties of galactic B[e] supergiants

IV. Hen 3–298 and Hen 3–303

A. S. Miroshnichenko[1,2,3], K. S. Bjorkman[1], M. Grosso[4], K. Hinkle[5], H. Levato[4], and F. Marang[6]

[1] Ritter Observatory, Dept. of Physics and Astronomy, University of Toledo, Toledo, OH 43606-3390, USA
e-mail: anatoly@physics.utoledo.edu
[2] Max-Planck-Institut für Radioastronomie, Auf dem Hügel 69, 53121 Bonn, Germany
[3] Central Astronomical Observatory of the Russian Academy of Sciences at Pulkovo, 196140 Saint-Petersburg, Russia
[4] Complejo Astronómico El Leoncito (CASLEO), Casilla de Correo 467, 5400 San Juan, Argentina
[5] National Optical Astronomical Observatories, PO Box 26732, Tucson, AZ 85726–6732, USA
[6] South African Astronomical Observatory, PO Box 9, Observatory 7935, South Africa

Received 18 January 2005 / Accepted 20 February 2005

Abstract. We present the results of optical and near-IR spectroscopic and near-IR photometric observations of the emission-line stars Hen 3–298 and Hen 3–303. Strong emission in the Hα line is found in both objects. The presence of Fe II and [O I] emission lines in the spectrum of Hen 3–298 indicates that it is a B[e] star. The double-peaked CO line profiles, found in the infrared spectrum of Hen 3–298, along with the optical line profiles suggest that the star is surrounded by a rotating circumstellar disc. Both objects also show infrared excesses, similar to those of B[e] stars. The radial velocities of the absorption and emission lines as well as a high reddening level suggest that the objects are located in the Norma spiral arm at a distance of 3–4.5 kpc. We estimated a luminosity of $\log L/L_\odot \sim 5.1$ and a spectral type of no earlier than B3 for Hen 3–298. Hen 3–303 seems to be a less luminous B-type object ($\log L/L_\odot \sim 4.3$), located in the same spiral arm.

Key words. stars: emission-line, B[e] – stars: individual: Hen 3–298 – stars: Hen 3–303 – techniques: spectroscopic – techniques: photometric – circumstellar matter

1. Introduction

The B[e] stars are a heterogeneous group. They are mostly of spectral type B with forbidden emission lines in their optical spectra and large IR excesses due to hot circumstellar (CS) dust (Allen & Swings 1976). Although a number of B[e] stars have either been identified as members of other known stellar groups (e.g., Herbig Ae/Be stars and Proto-Planetary Nebulae) or suggested to have high luminosities (B[e] supergiants, cf. Lamers et al. 1998), nearly half of the originally selected 65 galactic objects remained, until recently, unclassified.

Our studies of these unclassified objects resulted in identification of a new distinct group of B[e] stars with IRAS fluxes suggestive of a recent CS dust formation (hereafter B[e] stars with Warm Dust or B[e]WD, Miroshnichenko et al. 2002a). Analysis of their properties shows that they are neither pre-main-sequence nor post-asymptotic giant branch (post-AGB) objects. Nearly a quarter of B[e]WD were found to be detached binary systems, and a few more objects were suspected in binarity. Furthermore, their wide range of luminosities ($2.5 \leq \log L/L_\odot \leq 5.1$) and the location on the Hertzsprung-Russell diagram mostly within the main-sequence suggest that dust formation near hot stars can be much more common than originally thought. Most of the group members also exhibit very strong emission-line spectra, which indicate either a strong ongoing mass loss or the presence of a large amount of gas in their CS environments.

B[e]WD can be distinguished from other B[e] stars by the IR spectral energy distribution (SED). Analyzing the IRAS data of the originally selected B[e] stars, Miroshnichenko and collaborators noticed that 10 objects had specific colours ($-0.5 \leq \log(F_{25}/F_{12}) \leq 0.1$, $-1.1 \leq \log(F_{60}/F_{25}) \leq -0.3$, where F_{12}, F_{25}, and F_{60} are the fluxes in the IRAS photometric bands centered at 12, 25, and 60 μm, respectively) which correspond to dust temperatures of ≥150–200 K. Such colours are mainly characteristic of late-type stars with CS dust (symbiotic binaries, VV Cep binaries, Miras) and may indicate either the presence of a cool companion or a compact dusty envelope without cold dust. The latter may be due to a recent dust formation process. Cross-correlation of the IRAS Point Source Catalog (PSC) and the catalog of galactic early-type emission-line stars (Wackerling 1970) resulted in a finding of 11 more B-type stars with similar IRAS colours. Some of these objects were also selected by Dong & Hu (1991), who searched for optical counterparts from the same optical catalog to IRAS sources with strong

IR excesses ($V-[25] \geq 8$ mag, where V is the visual magnitude from Wackerling 1970 and [25] is the magnitude, calculated from the 25-μm IRAS flux). Initial studies of B[e]WD, listed by Dong & Hu (1991), were published by Miroshnichenko et al. (2000, 2001, 2002b).

The B[e]WD group includes a few high luminosity objects (e.g., CI Cam, CPD−52°9243, MWC 300, HDE 327083), similar to B[e] supergiants of the Magellanic Clouds (Zickgraf et al. 1986). The "hybrid" spectra of the latter (P Cyg type spectral line profiles in the UV region in combination with strong double- or single-peaked optical line profiles) have been explained in the framework of a two-component stellar wind model (dense and slow equatorial wind plus less dense and fast polar wind). First attempts have been made to explain dust formation around B[e] supergiants by Bjorkman (1998) and Kraus & Lamers (2003).

Our results on galactic B[e] supergiant candidates show that their luminosities are lower than was previously estimated. We found that their highest luminosities do not exceed $\log L/L_{\odot} = 5.1 \pm 0.2$ (see Miroshnichenko et al. 2001, 2003, 2004), while previous studies, which used limited observations (e.g., with no kinematical information), quoted higher values (e.g., 5.7 for MWC 300, Wolf & Stahl 1985 and 6.0 for HDE 327083, Machado & Araujo 2003). At the same time, B[e] supergiants have not been investigated thoroughly in the Milky Way. Thus observational studies of known, but yet poorly-studied early-type stars with IR excesses are important to reveal the population of dust-making galactic hot stars.

In this paper we present and analyze optical and IR observations obtained for two objects, Hen 3–298 = IRAS 09350−5314 and Hen 3–303 = IRAS 09369−5406, originally selected by Dong & Hu (1991) for their strong IR excesses, but previously unstudied. The observations are described in Sect. 2, our new results are presented in Sect. 3, our analysis of the observe properties is given in Sect. 4, and conclusions are summarized in Sect. 5.

2. Observations

Our optical spectroscopic observations were obtained at the 2.1 m telescope of the Complejo Astronómico El Leoncito (Argentina) with the échelle spectrograph REOSC, mounted at the Cassegrain focus and equipped with a 2000 × 2000 pixel CCD chip. This setup allowed us to achieve $R \sim 15\,000$. The log of our high-resolution spectroscopic observations is presented in Table 1. The data reduction was performed in IRAF[1].

Near-IR spectra were obtained at high-resolution ($R \sim 50\,000$) using the Gemini South telescope with the Phoenix spectrograph (Hinkle et al. 2003). Spectra of both Hen 3–298 and Hen 3–303 were obtained on 3 December 2002 in the 2.330 and 2.347 μm (4260 and 4290 cm^{-1}) region of the K band. Another spectrum of Hen 3–298 was obtained on 21 May 2004, with the same spectrograph, but with broader wavelength coverage from 2.304 to 2.347 μm (4260–4340 cm^{-1}). A detailed description of the observing and reduction process for Phoenix data taken at the same resolution and wavelength can be found in Smith et al. (2002). As in Smith et al. (2002), the telluric spectrum has been ratioed from the program star spectra by reference to a featureless hot star of similar airmass. The use of several hot reference stars and the radial velocity (RV) of the observed stellar features confirms that the observed emission lines in Hen 3–298 and Hen 3–303 are not absorption lines in the reference spectra. Details of the observations can be found in Table 1.

[1] IRAF is distributed by the National Optical Astronomy Observatories, which are operated by the Association of Universities for Research in Astronomy, Inc., under contract with the National Science Foundation.

Table 1. Log of high-resolution spectroscopic observations of Hen 3–298 and Hen 3–303. Listed are the object names, dates, exposure starting times (in MJD = JD−2 450 000), exposure time in seconds, spectral region in Å, signal-to-noise ratios (at 5900 Å for the optical spectra).

Object	Date	MJD	Exp.	Sp. region	*SNR*
Hen 3–298	2002/03/03	2336.744	1500	5600–8730	40
Hen 3–298	2002/04/15	2379.582	1800	5450–8415	40
Hen 3–298	2002/12/03	2611.830	180	23 343–23 450	150
Hen 3–298	2004/05/21	3146.613	720	23 061–23 179	100
Hen 3–298	2004/05/21	3146.569	720	23 163–23 279	200
Hen 3–298	2004/05/21	3146.545	720	23 264–23 378	250
Hen 3–298	2004/05/21	3146.508	720	23 367–23 479	250
Hen 3–303	2002/04/15	2379.608	1800	5450–8415	20
Hen 3–303	2002/05/22	2417.473	1500	5650–8750	20
Hen 3–303	2002/06/23	2449.462	1500	5650–8750	20
Hen 3–303	2002/12/03	2611.859	720	23 343–23 450	120

The near-IR broadband photometric observations were obtained at the 0.75-m telescope of the South-African Astronomical Observatory equipped with a single–element InSb photometer (Carter 1990). Additionally *JHK* data for the objects were extracted from the 2MASS catalog (Cutri et al. 2003). The photometric data are presented in Table 2.

The 2MASS survey detected 2 bright sources near the IRAS position of Hen 3–303 separated by ∼12″. Both sources are present in the GSC and USNO surveys with similar red magnitudes (∼13.1 mag in the GSC red band). They both were included in the aperture of the SAAO photometer (36″) and most likely were observed together by IRAS. However, the MSX (Egan et al. 2003) detected only one source with a high positional accuracy (∼0.″4). It coincides with the fainter 2MASS object (09383462–5420260). Also, the close IRAS and MSX fluxes suggest that the brighter 2MASS object (09383455–5420144) does not contribute to the mid-IR (8–60 μm) region. From its very red optical colour (the GSC blue–red colour-index ≥4 mag) and smaller 2MASS colour-indices, one can conclude that it is a cool star without a significant intrinsic IR excess.

3. Results

3.1. The spectrum

Optical and IR high-resolution spectroscopic observations were obtained for both objects for the first time. Optical spectra show that both Hen 3–298 and Hen 3–303 have extremely

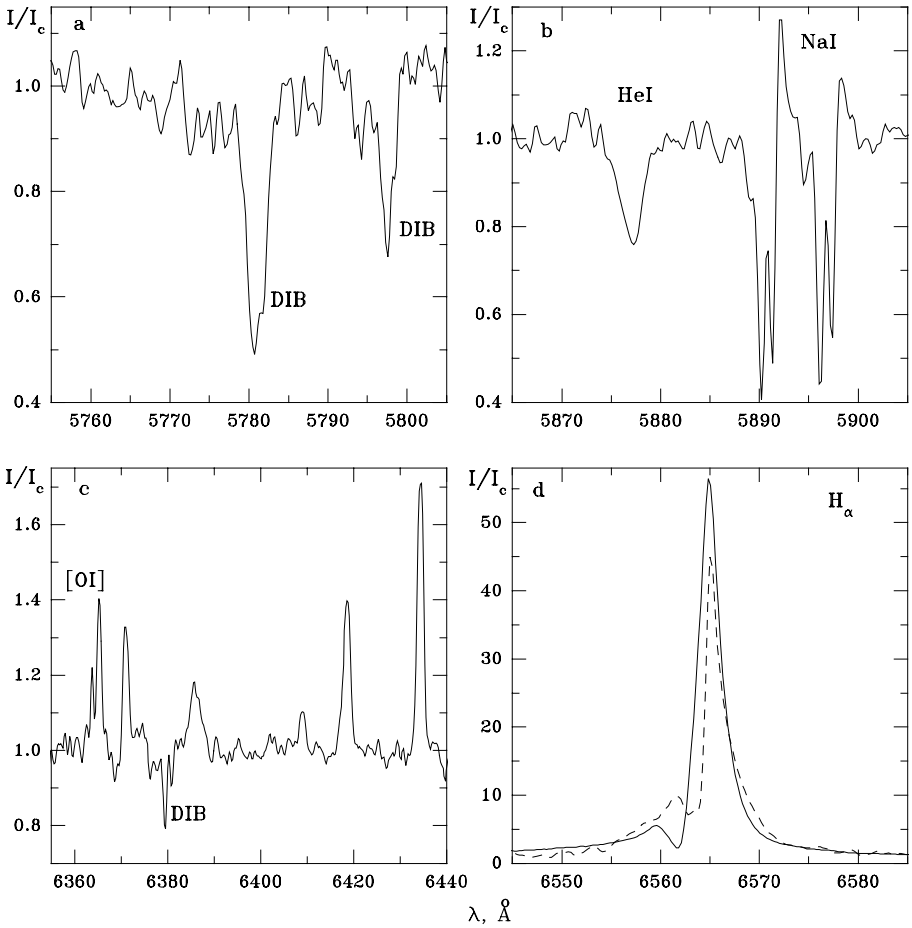

Fig. 1. Portions of the optical spectra of Hen 3–298 (solid lines). All unmarked lines in panel **c)** are Fe II lines. The Hα profile of Hen 3–303 is shown by the dashed line in panel **d)**. The intensities are in continuum units, and the wavelengths are in Å.

Table 2. Near-IR photometry of Hen 3–298 and Hen 3–303. Listed are the object names, observing dates, magnitudes, and sources of the data.

Object	JD 2 400 000+	*J*	*H*	*K*	*L*	Source
Hen 3–298	49 120.29	7.84 ± 0.03	6.80 ± 0.03	5.62 ± 0.03	3.94 ± 0.05	SAAO
Hen 3–298	51 586.59	7.85 ± 0.03	6.84 ± 0.06	5.70 ± 0.02	–	2MASS
Hen 3–298	52 033.29	7.95 ± 0.03	6.87 ± 0.03	5.66 ± 0.03	3.98 ± 0.05	SAAO
Hen 3–303[a]	49 120.31	8.46 ± 0.03	7.05 ± 0.03	6.32 ± 0.03	5.12 ± 0.05	SAAO
Hen 3–303[b]	51 553.79	8.55 ± 0.03	7.31 ± 0.06	6.77 ± 0.02	–	2MASS
Hen 3–303[c]	51 553.79	10.26 ± 0.03	8.89 ± 0.06	7.45 ± 0.03	–	2MASS
Hen 3–303[a]	52 033.32	8.48 ± 0.03	7.06 ± 0.03	6.31 ± 0.03	5.02 ± 0.05	SAAO

[a] Combined photometry of the 2MASS sources 09383455–5420144 and 09383462–5420260.
[b] Source 09383455–5420144 at RA $9^h38^m34\overset{s}{.}56$, Dec $-54°20'14\overset{''}{.}5$ (J2000).
[c] Source 09383462–5420260 at RA $9^h38^m34\overset{s}{.}63$, Dec $-54°20'26\overset{''}{.}0$ (J2000).

strong Hα lines (Fig. 1d) with double-peaked profiles and a stronger red peak. This is similar to most of the B[e]WD objects and indicates the presence of a flattened gaseous envelope around the objects.

The optical spectrum of Hen 3–298 contains many emission lines of Fe II with mostly single-peaked profiles. Along with the presence of the forbidden oxygen lines at 6300 and 6363 Å (Fig. 1c) and the Ca II IR triplet ($\lambda\lambda$ 8498, 8542, and 8662 Å), this indicates that Hen 3–298 is a typical B[e] star. The detected He I lines (at 5876 and 7065 Å) are in pure absorption, indicating a spectral type of no earlier than B3 (Fig. 1b). The width of the He I 5876 Å line ($FWHM \sim 140$ km s^{-1}) suggests that the star is not a rapid rotator. The Hα line varies in strength (the equivalent width is 220 Å in March and 140 Å in April 2002), but has the same position in our both spectra (central depression at -44 ± 1 km s^{-1}) with a peak separation of 244 ± 4 km s^{-1}. The strong Na I interstellar (IS) absorption lines and strong diffuse IS bands (DIB, Figs. 1a and 1b) imply a high level of IS reddening, supported by the available photometric data.

Table 3. Lines identified in the 2002/04/15 spectrum of Hen 3–298.

Line	λ_{lab}	EW	I/I_c	RV	Comment	Line	λ_{lab}	EW	I/I_c	RV	Comment
DIB	5780.41	1.69	0.49	30.3		FeII (74)	6456.38	1.01	1.68	80.4	dp
DIB	5849.80	0.29	0.70	46.3		FeII (40)	6516.05	1.42	1.91	85.2	
HeI (11)	5875.63	0.61	0.70	99.7	noisy	H I (1)	6562.82	0.00	3.72	−137.6	blue peak
NaI (1)	5889.95	0.73	0.16	15.4	blue comp	H I (1)	6562.82	140.00	39.10	102.8	red peak
NaI (1)	5889.95	0.38	0.27	75.0	red comp	H I (1)	6562.82	0.00	1.43	−43.5	cd
NaI (1)	5889.95	0.15	1.35	109.6	emis.	DIB	6613.62	0.52	0.61	15.8	blue comp.
NaI (1)	5895.92	0.57	0.20	14.9	blue comp	DIB	6613.62	0.24	0.78	74.7	red comp.
NaI (1)	5895.92	0.34	0.24	75.9	red comp	[FeII] (14F)	7155.14	1.22	1.93	85.0	
FeII (46)	5991.38	0.80	1.77	74.1		FeII (73)	7224.51	0.23	1.19	87.0	
FeII (46)	6084.11	0.32	1.24	75.9		[CaII] (1F)	7291.46	3.45	3.59	82.5	dp
FeII (74)	6238.38	0.96	1.45	101.7:	blend	[CaII] (1F)	7323.88	2.31	2.59	80.8	dp
FeII (74)	6247.56	0.97	1.48	66.5:	blend	FeII (73)	7449.34	0.50	1.24	84.6	dp
DIB	6283.86	2.20	0.42	37.5	noisy	[FeII] (14F)	7452.50	0.51	1.39	87.0	
[OI] (1F)	6300.23	0.91	1.89	85.4		FeII (73)	7462.38	0.93	1.42	84.5	dp
[OI] (1F)	6363.88	0.35	1.31	83.6		FeII (72)	7533.42	0.39	1.27	72.5	dp
FeII (40)	6369.45	0.38	1.31	70.3	dp	KI (1)	7698.98	0.33	0.56	15.8	
FeII (40)	6369.45	0.00	1.27	101.4		KI (1)	7698.98	0.13	0.81	86.4	
DIB	6379.20	0.28	0.74	15.6		FeII (73)	7711.71	1.55	1.71	83.5	
FeII (74)	6407.30	0.20	1.15	87.6	noisy	HI (11)	8323.43	0.79	1.30	82.3	
FeII (74)	6416.91	0.70	1.47	82.8		HI (11)	8333.79	0.96	1.31	86.1	
FeII (40)	6432.65	1.12	1.75	70.5	dp	HI (11)	8345.55	0.82	1.38	76.0	dp
FeII (40)	6432.65	0.00	1.71	98.9		HI (11)	8359.01	0.60	1.35	59.7	dp

Line ID is listed in Col. 1, its laboratory wavelength in Col. 2, equivalent width in Å in Col. 3, intensity in continuum units in Col. 4, heliocentric radial velocity in km s^{-1} in Col. 5, and a comment in Col. 6. Columns 7–12 repeat the information. Uncertain values are marked with a colon; dp stands for a double-peaked profile, cd for central depression.

The IR spectrum (Fig. 2) shows the presence of double-peaked CO emission lines, supporting the disc-like density distribution of the CS gas around Hen 3–298. Even a robust molecule line CO can not survive in the photosphere of a B star, conclusively demonstrating the CS origin of the CO emission line spectrum. CO lines can be identified from a number of vibration-rotational levels. Most of the lines from 2–0 R0 through 2–0 R 25 and 3–1 R17 through 3–1 R 40 can be identified. Those that are not identified are clearly present as blends. Our spectra do not cover the region from 2–0 R 26 to the 2–0 head at about R50 but the behaviour of the 3–1 lines and the strength of the observed 2–0 lines show that these lines would be easily observable.

The observed CO lines cover a range in excitation energy, hence the line strength normalized by the oscillator strength and statistical weight can be plotted as a function of excitation energy to give the rotational excitation temperature. The line equivalent widths suggest an excitation temperature of ~2000 K (Fig. 4). This exceeds the condensation temperature of most dust, suggesting that the CO spectrum originates in a dust free zone, near the dust sublimation region of the disc. The lines peak separation can be used to estimate the material rotational velocity (17.8 ± 0.4 km s^{-1}).

Unfortunately, the optical spectra of Hen 3–303, a fainter star, have a lower *SNR*. No emission lines, except the Hα, Ca II IR triplet, and traces of Fe II lines near 6400 Å were detected. The Hα line shows strength variations from 180 Å (April 2002) to 100 Å (June 2002) with the same position (central depression at 14 ± 3 km s^{-1} and a peak separation of 155 ± 5 km s^{-1}). The Na I IS absorptions are almost as strong as those in Hen 3–298 and also have two components (see Fig. 1b). No traces of CO bands were detected in the IR spectrum of Hen 3–303. The short interval of IR spectrum observed (Fig. 3) does have the Pfund hydrogen lines in emission. These lines are single peaked. From the three Pfund lines the velocity is +55 ± 2 km s^{-1}. The Paschen emission lines in the spectrum of Hen 3–303 show an RV of +80 km s^{-1}. The difference in RV between the optical and IR lines may be a sign of binarity. In any case, the combination of the SED of Hen 3–303 with the strong Hα emission suggest that it is also a B[e] star, a member of the B[e]WD group.

We derived RVs of different spectral lines in the spectrum of Hen 3–298. The mean heliocentric RV of the Fe II lines (from both optical spectra, see Table 1) is +83 ± 3 km s^{-1}. The He I and Paschen emission lines show the same velocity. The CO lines in the 2004 IR spectrum give the mean RV of +79 ± 0.4 km s^{-1}, in agreement with the optical data. Since the CO lines sample both sides of a rotating disc around the star, these lines should give an excellent measure of the stellar RV.

3.2. Spectral energy distribution

Henize (1976) gives visual magnitudes of 10.4 and 12.5 for Hen 3–298 and Hen 3–303, respectively. Beyond this, optical

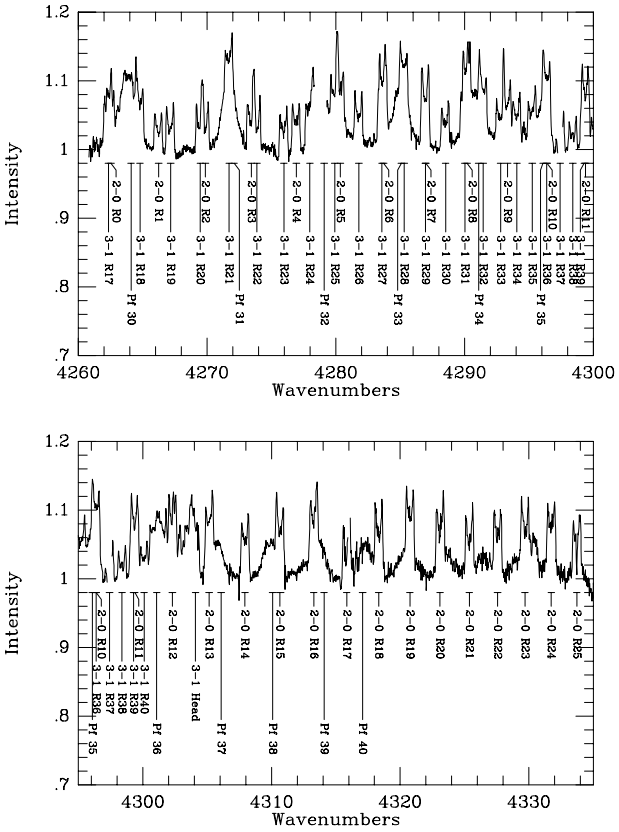

Fig. 2. The IR spectrum of Hen 3–298 observed at high resolution on May 21, 2004. The marked features are emission lines of the CO molecule originating from the 2–0 and 3–1 bands. Positions of the hydrogen lines of the Pfund series are also shown. The intensities are normalized to the continuum and the frequency scale is in cm^{-1}. In wavelength units the spectral region shown covers 2.3062 μm (4335 cm^{-1}) to 2.3468 μm (4260 cm^{-1}).

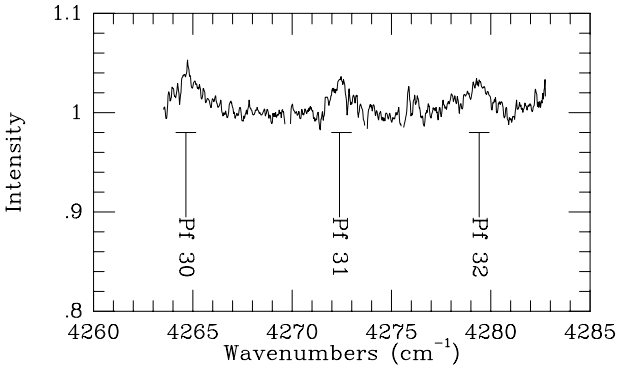

Fig. 3. The IR spectrum of Hen 3–303 observed at high resolution on December 3, 2002. The axes are as in Fig. 2. The hydrogen lines of the Pfund series are labeled. In wavelength units the spectral region shown covers 2.3343 μm (4283 cm^{-1}) to 2.3449 μm (4263 cm^{-1}).

photometric data on the program stars are available only from all-sky surveys (the Guide Star Catalog, Morrison et al. 2001; the USNO–B1.0 catalog, Monet et al. 2003). The *R*-band magnitudes from these surveys are 11.0 mag for Hen 3–298 and 13.1 mag for Hen 3–303. These optical brightnesses have uncertainties of the order of 0.4 mag, but show a consistent magnitude difference.

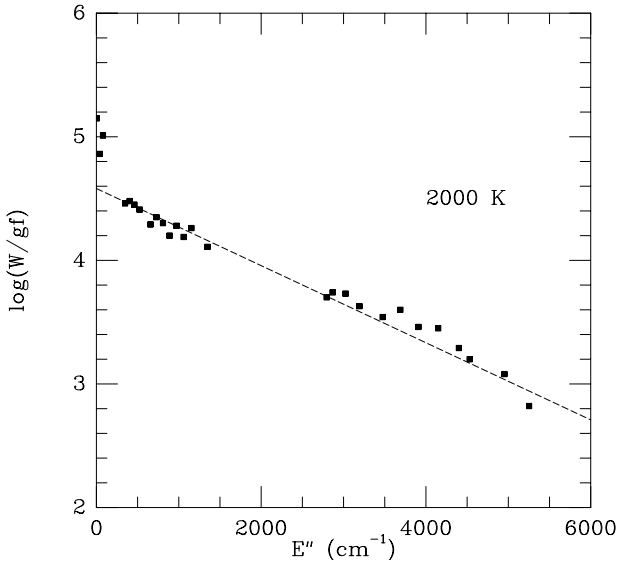

Fig. 4. Excitation temperature of the CO lines in the spectrum of Hen 3–298. The line equivalent widths normalized to the product of their statistical weight and oscillator strength are plotted versus the energy level in cm^{-1}.

We use the above visual magnitudes to normalize the SEDs shown in Fig. 5. The SEDs were corrected for the average galactic extinction law (Savage & Mathis 1979) with a $E(B-V) = 1.7$ mag for both objects. The reddening correction was applied so that the corrected *J*-band flux coincided with the theoretical model atmosphere. The accuracy of such a method is ~0.1–0.2 mag in $E(B-V)$ due to an uncertainty in the objects' spectral type and a possible contribution from the CS gas. However, experience with other B[e]WD shows that this gives consistent results compared to other methods (DIB strength, near-IR oxygen line ratio, e.g., Miroshnichenko et al. 2002b). Also, the IR excesses of both objects turned out to be similar to those of other B[e]WD (see Miroshnichenko et al. 2001).

There is a discrepancy of the derived $E(B-V)$ and that estimated from the strength of the DIBs (at 5780 and 5797 Å) in the spectrum of Hen 3–298 ($E(B-V) \sim 3$ mag) using a relationship from Herbig (1993). However, the relationship may not be linear for such strong DIBs. A different slope to this relation is also possible along the line of sight to the program objects. Thus, we consider the DIB method less reliable in this case.

The IR photometry clearly shows that both objects have strong IR excesses. The ground-based *JHKL* photometry is consistent with both the MSX and IRAS data (except in the case of the 2 sources observed together at SAAO). The IRAS LRS spectrum (Olnon et al. 1986) of Hen 3–298 is featureless. This is similar to those of most other B[e]WD and may indicate the dusty envelope is disc-like and have a large optical depth. The IRAS LRS spectrum of Hen 3–303, which is fainter in the 10-μm region than Hen 3–298, is very noisy.

4. Discussion

Our results show that both objects seem to be highly reddened B-type stars with significant IR excesses due to CS dust. The

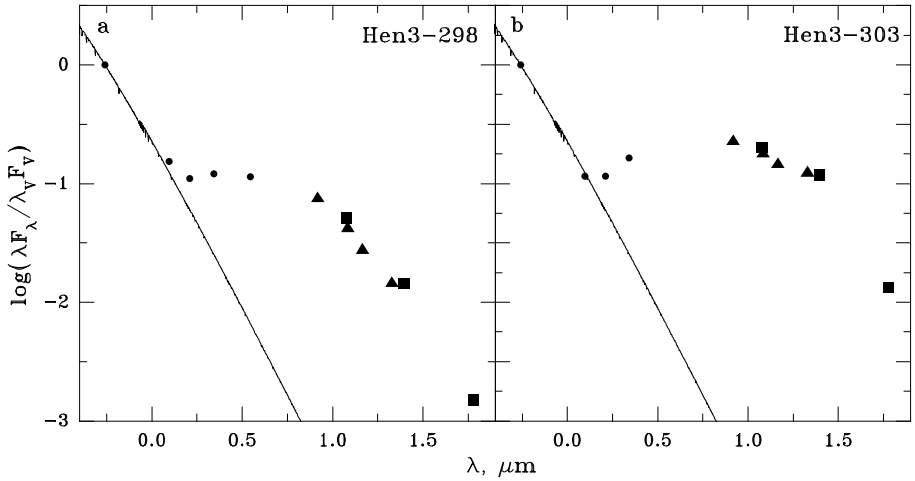

Fig. 5. The observed spectral energy distributions of Hen 3–298 (panel **a**)) and Hen 3–303 (panel **b**)) corrected for the IS extinction. The ground-based data are shown by filled circles, the MSX data (Egan et al. 2003) by filled triangles, the IRAS data by filled squares. The solid line represents the Kurucz (1994) theoretical model atmosphere for $T_{\rm eff}$ = 20 000 K, log g = 3.0. Refer to Sect. 4 for the IS reddening.

high reddening implies a large distance toward them. The IS extinction law in the objects' direction (Neckel & Klare 1980) suggests an extinction level of $A_{\rm V} \sim 1$ mag at distances $D \leq 2$ kpc followed by a linear increase further away from the Sun, so that the $A_{\rm V}$ exceeds 3 mag at $D \sim 4$ kpc.

From the constructed SEDs and the fact that B[e]WD show almost no excess radiation due to the CS envelope in the J-band, we estimated the overall (CS and IS) extinction for Hen 3–298 as $A_{\rm V} \sim 5.4$ mag. Hen 3–303 has a similar extinction. Part of the extinction may arise in CS medium.

The RV data suggest a large distance toward the objects, if we interpret them as due to the galactic rotation. According to Dubath et al. (1988), the heliocentric RV in this direction is only 25 km s^{-1} at 3 kpc. The rotation curve of these authors is not applicable to farther distances from the Sun.

The two strong IS components of the Na I doublet in the spectrum of Hen 3–298 and the two-component structure of some IS features (e.g., the DIB at 6613 Å and the K I line at 7699 Å) suggest the object may be located in the Norma spiral arm at D = 3–4.5 kpc. In this case the absolute visual magnitude of Hen 3–298 is $M_{\rm V} = -6.8 \pm 0.5$. In combination with a mid-B spectral type, it gives a $M_{\rm bol} \sim -8$ mag and a luminosity of $\log L/L_{\odot} \sim 5.1$. Thus, Hen 3–298 seems to belong to the highest luminosity subgroup of the B[e]WD, which contains such objects as MWC 300, HDE 327083, CI Cam, and Hen 3–1398.

The luminosity of Hen 3–303 is less certain, as we were not able to estimate its spectral type from our spectra. However, the observed reddening and RV suggest that Hen 3–303 is located in the same spiral arm as Hen 3–298. Taking into account the visual magnitude of ∼2 mag fainter than that of Hen 3–298, we can estimate a luminosity of Hen 3–303 to be $\log L/L_{\odot} \sim 4.3$. This estimate puts Hen 3–303 into the intermediate-luminosity subgroup of the B[e]WD, which includes MWC 342, MWC 623, MWC 657, AS 78, AS 160, and HD 85567.

The Hα line in both Hen 3–298 and Hen 3–303 has a central depression, which is blueshifted from the systemic RV by ∼120 and ∼100 km s^{-1}, respectively. On the other hand, the CO lines in the spectrum of Hen 3–298 are narrow and symmetric with respect to the systemic RV. This suggests that the CS gas distribution is dominated by an outflow in the inner regions of the gaseous envelope and by Keplerian rotation in the outer regions. Thus, the stellar wind slows down significantly not far from the hot star, where the material can accumulate, become dense enough to get shielded from the stellar UV photons, and thus form dust.

The objects are very unlikely to be young stars because the pre-main-sequence evolutionary time for B-type stars is too short (∼10^4–10^5 years, Palla & Stahler 1993) to get rid of the distant (and thus cold) protostellar dust. Observations of the most massive Herbig Be stars show that their IRAS fluxes at 60 and 100 μm are always larger than those at 12 and 25 μm. Hen 3–298 and Hen 3–303 do not seem to be post-AGB objects either due to reasons discussed by Miroshnichenko et al. (2000). Instead, they might recently left the main sequence and begun to form dust.

The high luminosity of Hen 3–298 and its strong emission-line spectrum may suggest that the object is a single B[e] supergiant, in whose slow and dense wind the dust may form (e.g., Kraus & Lamers 2003). On the other hand, there is strong evidence that most galactic B[e] supergiants are binary systems. The examples include recognized binaries, such as RY Sct (e.g., Gehrz et al. 2001) and HDE 327083 (Miroshnichenko et al. 2003), and a suspected one (MWC 300, Miroshnichenko et al. 2004).

It is harder to explain the existence of a strong wind in a lower-luminosity Hen 3–303, so that binarity might be more likely for it. Our previous results on B[e]WD (e.g., Miroshnichenko 2000, 2002b) show that the secondaries are 2–3 mag fainter than the primaries in the optical region and strongly call for additional high signal-to-noise spectroscopy of Hen 3–303. The RV difference in the optical and IR spectra, taken not contemporaneously, might be due to orbital motion. A lower systemic velocity does not contradict the location of the object in the Norma spiral arm. Also, the very strong

Hα emission is consistent with a B spectral type of the underlying star. Although our data are not sufficient to constrain its temperature, stars of later spectral types are unlikely to display such an emission-line spectrum.

5. Conclusions

Summarizing the results reported above, we can draw the following conclusions about the properties and nature of the emission-line objects Hen 3–298 and Hen 3–303.

1. Our high-resolution optical spectra show that both objects have strong line emission, similar to those of B[e]WD. The *RV*s of most of the emission and absorption lines suggest a large distance toward them. In combination with the photometric data, this suggests that the objects are located in the Norma spiral arm at a distance of 3–4.5 kpc.
2. The double-peaked profiles of optically-thick spectral lines (e.g., Hα) suggest a disc-like distribution of the CS gas near both objects. The double-peaked CO line profiles seen in the spectrum of Hen 3–298 also suggest such a distribution for the molecular part of the envelope. The featureless IRAS LRS of Hen 3–298 in the 10-μm region is consistent with a large optical depth of the dusty envelope, which most likely has a disc-like shape. The discs in both objects are viewed close to edge-on. The inclination of Hen 3–303 may be slightly steeper than that of Hen 3–298, so that the dust obscures the inner dissociation ring where CO originates.
3. Our estimate of the luminosity of Hen 3–298 ($\log L/L_\odot \sim 5.1$) suggests that it is among the highest luminosity galactic B[e]WD. Hen 3–303, with its smaller optical brightness, probably has a lower luminosity ($\log L/L_\odot \sim 4.3$).

As it was shown by Miroshnichenko et al. (2000, 2001, 2002b, 2003, 2004), almost all of the quoted above objects from the highest- and intermediate-luminosity subgroups of B[e]WD are either confirmed or suspected binaries. Thus, it is worthwhile to look for signs of binarity in both Hen 3–298 and Hen 3–303.

The following observations need to be performed in order to place stronger constraints on the objects' parameters. Optical photometry is needed to constrain the reddening and luminosity. High-resolution spectroscopy with higher *SNR* is needed to constrain spectral types and search for *RV* variations. Moderate resolution IR spectroscopy in the 10-μm region could reveal the chemical composition of the CS dust.

Acknowledgements. We thank T. Lloyd Evans for obtaining some of the near-IR photometric data at the SAAO and making them available to us. A.M. and K.S.B. acknowledge support from NASA grant NAG5–8054. We thank Dr. Robert Blum for assistance with the May 2004 Phoenix observations. This paper is based in part on observations obtained at the Gemini Observatory, which is operated by the Association of Universities for Research in Astronomy, Inc., under a cooperative agreement with the NSF on behalf of the Gemini partnership: the National Science Foundation (USA), the Particle Physics and Astronomy Research Council (UK), the National Research Council (Canada), CONICYT (Chile), the Australian Research Council (Australia), CNPq (Brazil), and CONICRT (Argentina). The observations were obtained with the Phoenix infrared spectrograph, which was developed and is operated by the National Optical Astronomy Observatory. The spectra were obtained through programs GS-2002B-Q-34 and GS-2004A-DD-1. This research has made use of the SIMBAD database operated at CDS, Strasbourg, France, as well as of data from the Two Micron All Sky Survey, which is a joint project of the University of Massachusetts and the Infrared Processing and Analysis Center/California Institute of Technology, funded by the National Aeronautics and Space Administration and the National Science Foundation.

References

Allen, D. A., & Swings, J.-P. 1976, A&A, 47, 293
Bjorkman, J. E. 1998, in B[e] stars, ed. A.-M. Hubert, C. Jaschek (Kluwer Acad. Publ.), 189
Carter, B. S. 1990, MNRAS, 242, 1
Cutri, R. M., Skrutskie, M. F., van Dyk, S., et al. 2003, CDS/ADC Collection of Electronic Catalogues, 2246
Dong, Y. S., & Hu, J. Y. 1991, Chin. A&A, 15, 275
Dubath, P., Mayor, M., & Burki, G. 1988, A&A, 205, 77
Egan, M. P., Price, S. D., Kraemer, K. E., et al. 2003, The Midcourse Space Experiment Point Source Catalog Version 2.3, October 2003, AFRL–VS–TR–2003–1589
Gehrz, R. D., Smith, N., Jones, B., Puetter, R., & Yahil, A. 2001, ApJ, 559, 395
Henize, K. G. 1976, ApJS, 30, 491
Herbig, G. H. 1993, ApJ, 407, 142
Hinkle, K. H., Blum, R. D., Joyce, R. R., et al. 2003, SPIE, 4834, 353
Kraus, M., & Lamers, H. J. G. L. M. 2003, A&A, 405, 165
Kurucz, R. L. 1994, Smithsonian Astrophys. Obs., CD-ROM No. 19
Lamers, H. J. G. L. M., Zickgraf, F.-J., de Winter, D., Houziaux, L., & Zorec, J. 1998, A&A, 340, 117
Machado, M. A. D., & Araújo, F. X. 2003, A&A, 409, 665
Miroshnichenko, A. S., Chentsov, E. L., Klochkova, V. G., et al. 2000, A&AS, 147, 5
Miroshnichenko, A. S., Levato, H., Bjorkman, K. S., & Grosso, M. 2001, A&A, 371, 600
Miroshnichenko, A. S., Bjorkman, K. S., Chentsov, E. L., & Klochkova, V. G. 2002a, in Exotic Stars as Challenges to Evolution, ed. C. A. Tout, & W. Van Hamme, ASP Conf. Ser., 279, 303
Miroshnichenko, A. S., Bjorkman, K. S., Chentsov, E. L., et al. 2002b, A&A, 383, 171
Miroshnichenko, A. S., Levato, H., Bjorkman, K. S., & Grosso, M. 2003, A&A, 406, 673
Miroshnichenko, A. S., Levato, H., Bjorkman, K. S., et al. 2004, A&A, 417, 731
Monet, D. G., Levine, S. E., Canzian, B., et al. 2003, AJ, 125, 984
Morrison, J. E., Roeser, S., McLean, B., Bucciarelli, B., & Lasker, B. 2001, AJ, 121, 1752
Neckel, Th., & Klare, G. 1980, A&AS, 42, 251
Olnon, F. M., Raymond, E., & the IRAS Science Team 1986, A&AS, 65, 607
Palla, F., & Stahler, S. W. 1993, ApJ, 418, 414
Savage, B. D., & Mathis, J. S. 1979, ARA&A, 17, 73
Smith, V. V., Hinkle, K. H., Cunha, K., et al. 2002, AJ, 124, 3241
Thé, P. S., de Winter, D., & Pérez, M. R. 1994, A&AS, 104, 315
Wackerling, L. R. 1970, Mem. RAS, 73, 153
Wolf, B., & Stahl, O. 1985, A&A, 148, 412
Zickgraf, F.-J., Wolf, B., Leitherer, C., Appenzeller, I., & Stahl, O. 1986, A&A, 163, 119